Modeling and Evaluation of Power System Behavior with Mechanical System

Yuko Omagari† and Tsuyoshi Funaki†

†Division of Electrical, Electronic and Information Engineering, Osaka University
1-2 Yamadaoka, Suita, Osaka, 565-0871 Japan
Email: yuko@ps.eei.eng.osaka-u.ac.jp, funaki@eei.eng.osaka-u.ac.jp

Abstract– A power system is a nonlinear dynamical system. Understanding the dynamic behavior of a power system is necessary for its reliable operation. K. Noda proposed an equivalent mechanical model of a power system to help intuitively understanding power system behavior obtained from a mathematical model of a power system. The validity of the mechanical model was confirmed qualitatively. This study quantitatively evaluates the mechanical model through experiments that assess the accuracy of its analogy with the mathematical model. To this end, the steady-state and transient stability limit of a power system are demonstrated. The limitation on the mechanical-mathematical model analogy is evaluated.

1. Introduction

A power system is a nonlinear dynamical system. Stability of a power system significantly influences the reliability of its operation. Even smart grids cannot avoid stability problems, because their configuration is similar to that of conventional power systems. For the successful operation of a power system, it is necessary to understand the phenomena arise in a power system involved with power system stability.

Traditionally, power system stability has been associated with generator rotor angle dynamics, which are described by a second-order differential equation. Power system stability is analytically studied on the basis of this mathematical model of a power system. However, intuitively understanding the power system behavior obtained from the stability study is difficult because electricity is invisible.

A mechanical model of a power system may help understand power system behavior by representing it visually. K. Noda proposed a mechanical model of a two-machine power system, which consists of a rotating mass and spring [1]. The validity of the mechanical model was qualitatively confirmed on the basis of the mathematical expressions of the mechanical and mathematical power system models [1]. Furthermore, the quantitative validation of the mechanical model was performed to assess the accuracy of its analogy with the mathematical model, because the electric components in a power system are represented by the mechanical components in the mechanical model [2]. The error of the mechanical model occurs due to springs [2]. In this study, springs are specially wound to have the length proportional with the spring tension for eliminating the error stemming from a finite natural length of spring. The mechanical model with these springs is quantitatively evaluated through experiments. The accuracy of the mechanical-mathematical model analogy is assessed. To this end, the steady-state and transient stability limit of a power system in the mechanical model is demonstrated. The limitation on the application of the mechanical model to represent power system behavior is provided.

2. Power System Behavior

Figure 1 shows a single-phase equivalent circuit of a two-machine power system. This simplest system is useful in describing the basics of power system behavior. Power system stability is studied for this system.

2.1. Mathematical Model of Two-machine Power System

The dynamics of a synchronous generator are governed by the following second-order differential equation.

$$M\frac{d^2\delta}{dt^2} + D\frac{d\delta}{dt} = P_m - P_e \qquad (1)$$

Where, M is the inertia constant, δ is the rotor angular displacement with respect to the synchronously rotating reference, and D is the damping coefficient. P_m and P_e are the mechanical power input and the electrical power output of a generator, respectively.

For the two-machine power system, the real and reactive powers at the generator are given as functions of phase angle δ.

$$P_e = \frac{V_G V_M}{X}\sin\delta, \quad Q_e = \frac{V_G^2 - V_G V_M \cos\delta}{X} \qquad (2)$$

The power–angle (P_e–δ) characteristic in (2) gives nonlinearity in the power system operation.

2.2. Power System Stability

Interconnected synchronous machines in a power system are required to operate in synchronism when subjected to

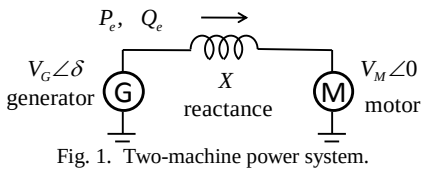

Fig. 1. Two-machine power system.

disturbance, and the ability to achieve this is called power system stability. This stability is typically classified into steady-state and transient, depending on the severity of disturbance [3]. The former is the local stability and the latter is the global stability.

2.2.1. Steady-state Stability

Steady-state stability is the ability of a power system to maintain synchronism when subjected to small disturbance such as gradual change in load. The steady-state stability can be studied by linearizing (1) about an operating point [4].

For simplicity, the two-machine power system of Fig. 1 is integrated into a single-machine and infinite bus system. Linearizing (1) for constant P_m and negligible damping effect, we get

$$M\frac{d^2\Delta\delta}{dt^2} = -\frac{dP_e}{d\delta}(\Delta\delta), \tag{3}$$

where Δ denotes a small deviation.

The system is stable in the range of $\delta \le 90°$: both roots of (3) are on the imaginary axis, where δ oscillation does not diverge. The system is unstable in the range of $\delta > 90°$: both roots are real, positive and negative, and δ results in divergence. At $\delta = 90°$, the system is at the stability limit. The steady-state stability power limit is

$$P_{\max} = \frac{V_G V_M}{X}. \tag{4}$$

2.2.2. Transient Stability

Transient stability is the ability of a power system to maintain synchronism when subjected to large disturbance, such as a short-circuit fault on a transmission line. There are two commonly used methods for a transient stability study: time-domain simulation and energy function method. In the time-domain simulation method, (1) is solved numerically to discriminate whether the rotor angle increases indefinitely or oscillates and converges to an equilibrium point. The energy function method is a special case of the Lyapunov's second method and is applied to the transient stability study as follows [5].

Recognizing that $P_e = P_{\max}\sin\delta$, the energy function $V(\delta, \omega)$ of the system for (1) is defined as

$$V(\delta,\omega) = \frac{1}{2}M\omega^2 + \int_{\delta^s}^{\delta}\left(-P_m + P_{\max}\sin\delta\right)d\delta, \tag{5}$$

where $\omega = d\delta/dt$. Note that the damping component in (1) is neglected. The first term is kinetic energy and the second is potential energy, and δ^s is the post-disturbance stable equilibrium point. The critical energy V_{cr} at the stability boundary is equal to the system potential energy at the post-disturbance unstable equilibrium point δ^u.

The transient behavior of a single-machine infinite bus system is studied for a local load shedding. When the mechanical power input suddenly increases from an initial value of P_{m0} to P_m, which is equivalent to a local load shedding, there is surplus of mechanical power input over electrical power output. The post-disturbance stable δ^s and unstable δ^u equilibrium points are given by

$$\delta^s = \arcsin\left(\frac{P_m}{P_{\max}}\right), \quad \delta^u = \pi - \delta^s. \tag{6}$$

The initial conditions at the onset of the disturbance are $\omega = 0$ and $\delta = \delta_0$, where δ_0 is the operating point before the onset of disturbance. Then, the energy V_s of the system is $V_s = V(\delta_0, 0)$. The critical energy V_{cr} at the stability boundary of the system is $V_{cr} = V(\delta^u, 0)$.

If V_s is less than V_{cr}, then the system is stable; if it is greater, then the system is unstable, that is, δ diverges and the generator falls out of step. At $V_s = V_{cr}$, the system is at the stability limit and we get the following relationship.

$$\cos\delta_0 - \cos(\pi - \delta^s) = (\pi - \delta^s - \delta_0)\sin\delta^s \tag{7}$$

Solving (7) for δ^s, the maximum local load shedding $\Delta P_{\max}$ is given by

$$\Delta P_{\max} = P_{\max}\sin\delta^s - P_{m0}. \tag{8}$$

3. Equivalent Mechanical Model of Power System

This section briefly reviews the mechanical model of the two-machine power system. The qualitative analogy between the mechanical and the mathematical models is derived on the basis of the correspondence in their mathematical expressions. Then, the behavior of the power system in the mechanical model is illustrated. The details are covered in [2].

3.1. Mechanical Model of Two-machine Power System

Figure 2 shows the schematic diagram of the mechanical model of the two-machine power system developed by K. Noda [1]. Rotating disks G and M represent the generator and motor, respectively. They pivot independently on a common axis and are interconnected by three springs. The three springs are equiangularly placed on the fringe of the disks to represent a balanced three-phase system. The rotating handle and weights represent mechanical power input and output of the generator and motor, respectively.

The physical parameters of the mechanical model are summarized in Table I. In this study, springs are fabricated so that they have a proportional relationship between the

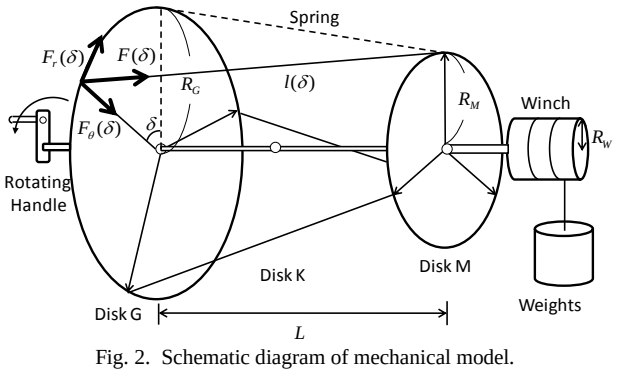

Fig. 2. Schematic diagram of mechanical model.

TABLE I. PHYSICAL PARAMETERS OF MECHANICAL MODEL

disk radius: R_G, R_M	7.30×10^{-2} [m]
winch radius: R_W	2.50×10^{-2} [m]
distance: L	2.45×10^{-1} [m]
combined moment of inertia of disk M and winch: J	7.36×10^{-4} [kg·m^2]
dynamic friction torque of disk M: μ	2.99×10^{-4} [N·m]
maximum static friction torque of disk M	6.1×10^{-4} [N·m]

spring tension and the spring length [2] to eliminate the errors due to a finite natural length of spring. The relationship between the spring tension $F(\delta)$ [N] and the spring length $l(\delta)$ [m] is measured as $F(\delta) = 8.67 \times l(\delta)$.

3.2. Analogy of Mechanical Model with Mathematical Model

The dynamics of the disk are governed by the following second-order differential equation.

$$J \frac{d^2\delta}{dt^2} + \mu = T_m - T_e \tag{10}$$

Where, J is the moment of inertia of the disk and T_m and T_e are the torques acting on the disk originating from the rotating handle or weights and from the spring tension, respectively. μ is the dynamic friction torque and δ is the displacement angle between the two disks. By comparing (10) with (1), correspondence between parameters and variables are found.

The mechanical–mathematical model analogy proposed by K. Noda is described [6]. The spring length is expressed as a function of δ.

$$l(\delta) = \sqrt{L^2 + (R_M \sin\delta)^2 + (R_G - R_M \cos\delta)^2} \tag{11}$$

Where, R_G and R_M are radii of disks G and M, respectively, and L is the distance between the two disks.

The spring tension $F(\delta)$ acting on disk G can be decomposed into tangential $F_r(\delta)$ and centripetal $F_\theta(\delta)$ components. The product of $F_r(\delta)$ and R_G gives the torque $T_r(\delta)$ acting on disk G. Similarly, the product of $F_\theta(\delta)$ and R_G gives the imaginary torque $T_\theta(\delta)$.

$$T_r(\delta) = \frac{R_G R_M \sin\delta}{S}, T_\theta(\delta) = \frac{R_G^2 - R_G R_M \cos\delta}{S} \tag{12}$$

Where, $S \equiv l(\delta)/ F(\delta)$. When $F(\delta)$ is proportional to $l(\delta)$, $S = 1 / k$ where k is a spring constant.

Comparing (12) with (2), the following correspondence exists between the parameters and variables in the mechanical and mathematical power system models:

- Radii R_G and R_M correspond to voltages V_G and V_M, respectively.
- Torque $T_r(\delta)$ corresponds to real power P_G.
- Imaginary torque $T_\theta(\delta)$ corresponds to reactive power Q_G.
- The reciprocal of sprig constant S corresponds to transmission line reactance X.

Thus, the analogy between the mechanical and mathematical power system models is clearly shown, on the basis of the correspondence of their differential and algebraic equations.

3.3. Behavior of Power System in Mechanical Model

The behavior of a power system subjected to small disturbance is simulated in the mechanical model as follows. As weight is added in small increments, torque T_r increases and disk M rotates with δ gradually increasing from 0°. T_r reaches its maximum value at δ = 90°. As more weight is added, the torque due to the weight acting on disk M will not balance T_r. Then, disk M is accelerated and δ increases, resulting in three springs intersecting at the midpoint. The corresponding power system is unstable. The maximum torque obtained in this manner corresponds to the steady-state stability power limit of a power system.

The mechanical model can also simulate the transient behavior of a power system following local load shedding. An abrupt load change is simulated by suddenly adding a large weight ΔW. If ΔW is small, disk M rotates and stops at a new equilibrium point. If ΔW is very large, disk M is accelerated and δ increases indefinitely, resulting in the three springs intersecting at the midpoint. The maximum increase in torque obtained in this manner corresponds to the maximum local load shedding of a power system.

4. Results and Discussion

This section quantitatively evaluates the mechanical model with the mathematical model by a comparative study on the steady-state stability power limit and the maximum local load shedding.

4.1. Experiment Results

4.1.1. Mechanical Experiment Results

The steady-state stability power limit and the maximum local load shedding in the mechanical model are experimentally obtained as in Section 3.3. The maximum local load shedding is conducted for different initial conditions δ_0 of 20.0° and 40.0° in the mechanical experiment. The results are shown in Table II.

4.1.2. Numerical Experiment Results

The parameters of the mathematical model are set to be equivalent to the physical parameters of the mechanical model. The steady-state stability power limit and the maximum local load shedding in the power system model are obtained as in Section 2.2. The maximum local load shedding is evaluated with the energy function method for different initial conditions δ_0 of 20.0° and 40.0°. The Newton–Raphson method is used to solve (7). The maximum local load shedding is also evaluated with the time-domain analysis for respective δ_0 to allow for the damping effect. Equation (1) is solved by the fourth-order Runge–Kutta method with a time step of 0.01 sec. The results are shown in Table II.

TABLE II
MECHANICAL AND NUMERICAL EXPERIMENTS RESULTS

		mechanical simulator [pu[*1]]	mathemtaical model [pu[*2]]	
steady-state stability power limit		4.8	4.6	
maximum local load shedding	δ_0=20.0°	2.4	2.2[*3]	2.3[*4]
	δ_0=40.0°	1.5	1.2[*3]	1.3[*4]

[*1] 1 [pu] = 1×10^{-2} [N·m], System base = 100 [MVA], Voltage base = 500 [kV], $V_G = V_M = 1$ [pu]
[*2] X = 0.216 [pu], M = 7.63 [MJ/rad] and D = 2.99, [*3] energy function method, [*4] time-domain analysis

4.2. Discussion

4.2.1. Steady-state Stability

The error of the mechanical model to the mathematical model is 4.3 [%]. The error can be caused by the static friction torque. When the static friction torque (0.061 [pu]) is considered, the error reduces to 3.0 [%]. Because the error is small, within a few percent, the mechanical model validly represents the steady-state stability power limit of a power system.

4.2.2. Transient Stability

The mechanical model provides the higher maximum local load shedding than the mathematical model. The error of the mechanical simulator for the initial condition of δ_0 = 20.0° and 40.0° are 9.1 and 25 [%], respectively. Because the error is large, it is not quantitatively validated.

The error of the mechanical simulator can be attributed to the dynamic friction torque which is not considered in the numerical experiment with the energy function method. When the dynamic friction torque is considered, the errors for δ_0 = 20.0° and 40.0° reduce to 4.3 and 15 [%], respectively. However, a large error remains for a large δ_0. This may be attributed to the static friction torque in the mechanical model. The influence of the friction on the behavior of the mechanical model is difficult to evaluate and the static friction torque is not considered in the mechanical model equation and in the discussion of the analogy.

Because the error of the mechanical model at δ_0 = 20.0° is small, within a few percent, the mechanical model is quantitatively validated for a small δ_0. However, the error in the mechanical model occurs due to the friction torque.

5. Conclusions

Because electricity is invisible, it is difficult to intuitively understand the power system behavior obtained from a stability study. In this study, we described the mechanical model of a power system, which provides a means of visualizing power system behavior. The qualitative analogy between the mechanical and mathematical power system models was derived, on the basis of the correspondence in their mathematical expressions.

In this study, springs were fabricated so that the spring tension was proportional to the spring length in order to eliminate the error of the mechanical model due to a finite natural length of spring. A quantitative evaluation of the mechanical model with the developed springs was performed by comparing the mechanical experiment results with the numerical experiment results of the mathematical model. The mechanical model was quantitatively validated in expressing the steady-state stability power limit. However, the error of the mechanical model stemming from the dynamic friction torque still remained in demonstrating the maximum local load shedding. The error was reduced with considering the dynamic friction torque and the mechanical model was quantitatively validated for initial operating point with small power angle.

The mechanical model can be used to aid in intuitively understanding power system behavior and the concept of power system stability.

Acknowledgments

The authors would like to thank K. Noda for his useful comments on this study.

References

[1] K. Noda, "Equivalent mechanical model of a power system for understanding ac transmission system," in *Proc. the 1973 Annual Meeting of IEEJ*, p. 1205, 1973 (in Japanese).
[2] Y. Omagari and T. Funaki, "Experimental validation of equivalent mechanical model for understanding dynamical behavior of power systems", *NOLTA, IEICE*, vol. E94-N, no.7, July, 2011.
[3] P. Kundur, *Power system stability and control*, New York: McGraw-Hill, 1994.
[4] e.g. N. Uchida and T. Nagano, "Eigenvalue analysis of very large power systems," *IEEE Trans. Power syst.*, vol. 3, no. 2, pp. 472-480, 1988.
[5] e.g. P.C. Magnusson, "The transient energy method of calculating stability," *AIEE Trans.*, vol. 66, no. 1, pp. 747-755, 1947.
[6] K. Noda ed., *Power control and information series Power System Control*, Tokyo: Denkishoin, 1986 (in Japanese).